Enhancing pro-inflammatory glioma-associated myeloid cells and CD8$^+$ T cells via hypoxia reduction

Glioblastoma (GBM) tumors contain a harsh immune environment consisting of anti-inflammatory glioma-associated myeloid-derived suppressor cells/ macrophages/microglia (GAMs) and reduced cytotoxic CD8$^+$ T cells. Tumor hypoxia exacerbates this immunosuppressive microenvironment by creating a physical barrier for the infiltration of CD8$^+$ T cells into the tumor core. Moreover, while CD8$^+$ T cells need high metabolic energy states to function, hypoxia fosters a hostile tumor microenvironment (TME) that suppresses infiltrating CD8$^+$ T cells by inducing metabolic dysfunction. GAMs adapt to this low-oxygen environment by upregulating the hypoxia-inducible factor (HIF) pathway. This polarizes them towards a pro-tumor M2 phenotype which subsequently inhibits pro-inflammatory responses. As a result, this immunosuppressive TME may be reprogrammed to a pro-inflammatory phenotype upon the reversal of tumor hypoxia. Therefore, my project focuses on identifying the impact of tumor hypoxia reduction on the distribution and functionality of CD8$^+$ T cells and GAMs in the TME. Previous research from our lab has shown that the hypoxia-activated prodrug, [redacted], reduces tumor progression by diminishing immunosuppressive myeloid-derived suppressor cells and reducing CD8$^+$ T cell suppression in a checkpoint blockade-resistant prostate cancer model. Consequently, we aim to elucidate the potential of [redacted] in reshaping the immune landscape within GBM tumors by targeting hypoxia-induced immunosuppressive mechanisms. As a result, **we hypothesize that hypoxia reduction enhances the anti-tumor immune response by promoting CD8$^+$ T cell infiltration and cytotoxicity and repolarizing immunosuppressive GAMs within the TME.** To test our hypothesis, we have outlined the following objectives:

Aim 1: Determine the effects of hypoxia reduction on CD8$^+$ T cell distribution, infiltration, and cytotoxicity in GBM.

There is limited information on the impact of hypoxia reduction on CD8$^+$ T cell distribution, metabolism, and functionality in GBM tumors. We hypothesize that hypoxia reduction in GBM creates a more conducive environment for CD8$^+$ T cell trafficking from the lymph nodes (LNs), and metabolically rewires them within the TME to enhance their cytotoxic function. The hypoxic niche will be characterized by measuring *in vivo* hypoxia levels using 18F-FAZA PET imaging in GL261 GBM tumor-bearing mice with/without [redacted]. The spatiotemporal distribution of T cells will be visualized using immunofluorescence (IF) imaging in GBM tumors with/without [redacted]. The impact of hypoxia reduction on the T cell metabolic capacity will be assessed using a seahorse assay. This will measure the oxygen consumption rate in *ex vivo* CD8$^+$ T cells isolated from GBM tumors with/without [redacted]. CD8$^+$ T cell activation, proliferation, cytotoxicity, and exhaustion will be assessed using flow cytometry on primary lymphocytes isolated from tumor-draining lymph nodes (TdLNs) and tumors of tumor-bearing mice with/without [redacted]. Finally, to study the impact of hypoxia reduction on T cell trafficking from the TdLNs, FTY720, an S1P receptor antagonist, will be used to block T cell egress from the LNs of tumor-bearing mice with/without [redacted]. The subsequent impact on the immune response in the TME will be identified by analyzing tumor infiltrating CD8$^+$ T cells for their activation, proliferation, and cytotoxicity using flow cytometry.

Aim 2: Discern the impact of hypoxia reduction on the distribution and polarization of GAMs in GBM.

Tumor hypoxia is known to enhance immunosuppressive M2 macrophages within the TME. However, the impact of tumor hypoxia reversal on GAM subtypes in GBM remains unclear. We hypothesize that hypoxia reduction repolarizes immunosuppressive M2 GAMs towards an M1 phenotype by inhibiting downstream HIF signaling, subsequently diminishing their capacity to suppress CD8$^+$ T cells. To test this, the spatiotemporal distribution of GAMs will be characterized using IF imaging of GBM tumors with/without [redacted]. The impact of hypoxia reversal on GAM phenotype and functionality (M1 or M2) will be assessed via flow cytometry on GAMs isolated from GBM tumors with/without [redacted]. The impact of [redacted] on GAM transcriptional programming will be assessed using bulk RNA sequencing of GAMs isolated from primary tumors with/without [redacted]. Emphasis will be placed on HIF expression. The role of HIF signaling in guiding GAM polarization post-hypoxia reduction will be studied using mouse models with myeloid-specific knockout of HIF1α or HIF2α with/without [redacted] using flow cytometry. To test the impact of GAM repolarization on the antigen-specific T cell response, a co-culture will be used. Primary GAMs isolated from GBM OVA tumors with/without [redacted] will be co-cultured with naïve OT-1 CD8$^+$ T cells. CD8$^+$ T cells will be assessed via flow cytometry for proliferation and cytokine production. Additionally, GAMs will be analyzed via flow cytometry for markers linked to enhanced T cell suppression under hypoxia (inhibitory molecules, molecules depleting essential amino acids, and immunosuppressive cytokines).

Hypoxia is a detrimental factor suppressing the immune response initiated by standard therapies in GBM. Understanding the effect of hypoxia reduction on the dominant immune pathways in GBM is indispensable for improving the efficacy of antitumor drugs and enhancing the prognosis of GBM which poses an overwhelming public health burden.

SIGNIFICANCE

Glioblastoma (GBM) is the most malignant and aggressive glioma that accounts for 49% of primary brain tumors, with a median survival of around 1 year following diagnosis[1]. Despite surgical resection and multimodal treatment with radiation and chemotherapy temozolomide, 70% of GBM patients experience disease advancement one year after diagnosis[2]. Thus, better therapeutic strategies for the clinical management of GBM are direly needed. Tumor hypoxia induces resistance to conventional therapies by hindering the body's ability to mount an effective anti-tumor immune response[1]. Rapidly proliferating cancer cells have high metabolic demands, using up oxygen and metabolites for their growth and survival[3]. This depletes the tumor microenvironment (TME) of oxygen and vital nutrients for immune functioning, thereby hindering the immune response. As a result, tumor hypoxia impedes the survival of cytotoxic immune cells while promoting the survival of immunosuppressive cells[1],[3]–[5]. Hypoxia is a key biomarker of survival in GBM, with higher hypoxic volume correlating to lower overall and progression-free survival[6]. This highlights the importance of studying tumor hypoxia reduction and understanding its impact on immune cell functioning to improve patient outcomes in GBM.

Hypoxic tumor cells under the control of HIF signaling release chemokines such as stromal cell-derived factor 1 α (SDF1α), CCL2, semaphorin 3A (Sema3A), monocyte chemoattractant protein-1 (MCP-1), and vascular endothelial growth factor (VEGF) that draw immature monocytes toward the hypoxic niche[7],[8]. Once they infiltrate tumor hypoxic zones, they lose receptors to these chemokines, get trapped, and are converted to more immunosuppressive TAMs and MDSCs[9]. As a result, these monocytes adapt to this hypoxic environment by upregulating hypoxia-inducible factors, HIF-1α and HIF-2α[10]–[12]. While HIF-1α and HIF-2α have differential roles in inducing GAM polarization (HIF-1α induces M1 and HIF-2α induces M2 macrophages), they trigger downstream pathways that shift the balance towards an increased presence of immunosuppressive M2 macrophages. Yet, the process of attracting monocytes and inducing immunosuppression is not clearly understood in GBM where GAMs make up 50% of the immune cell milieu. Additionally, there is limited information on the impact of hypoxia reversal on the GAM subset, brain-resident microglia, that are found exclusively in the central nervous system.

Hypoxic stress impairs the infiltration of cytotoxic $CD8^+$ T cells by creating physical barriers that restrict their entry into the tumor core[14], [15]. The cytotoxic immune cells that do manage to enter the hypoxic core are inhibited by a myriad of metabolic stressors that are often the direct effect of hypoxia (nutrient and oxygen insufficiency, immunosuppressive cytokines, and inhibitory checkpoint receptors). As a result, these $CD8^+$ T cells undergo metabolic alterations that suppress their cytotoxic functionality [16],[17]. While previous literature has established the need for sustained glycolysis for T cell activation and proliferation, research by Sharping et al highlighted that $CD8^+$ T cells under hypoxia have diminished mitochondrial function[18]. This reduces oxidative metabolism and subsequently hampers their effector function and persistence[18]. Therefore, both pathways of metabolism (glycolysis and oxidative phosphorylation) are required for the efficient activation and functionality of T cells. In summary, tumor hypoxia creates a hostile environment that promotes the presence of anti-inflammatory M2 GAMs and inhibits cytotoxic $CD8^+$ T cells, which together hinder antitumor immune functions.

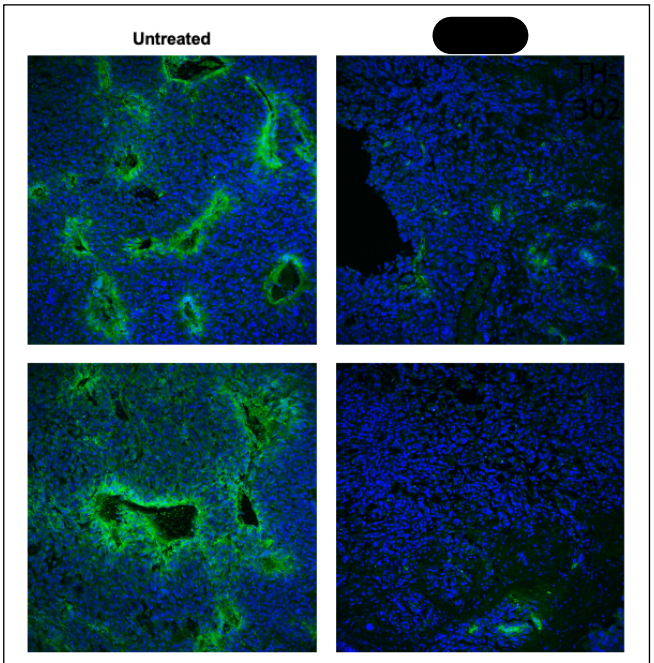

Figure [redacted] reduces hypoxia in GL261 Tumors
GL261 GBM tumor-bearing mice were treated with a single cycle of [redacted] (days 14-19) and stained for hypoxia following pimonidazole injection (Hydroxyprobe) on day 30. Brain sections were imaged at 10x magnification using the Leica SP8 Confocal Microscope. Representative images are shown for each group. Blue – DAPI, Green – Hypoxia.

Although these mechanisms are better defined in other tumor models, there is limited information regarding the influence of hypoxia reduction on GAM polarization, and $CD8^+$ T cell infiltration, metabolic alterations, and functionality in GBM. While standard GBM treatment aims to eliminate tumor cells and stimulate the activity of immune cells, its effectiveness is inhibited by hypoxia. This highlights the importance of addressing tumor hypoxia in the treatment of GBM. Understanding these complex immune cell pathways and interactions is vital for enhancing the efficacy of cancer immunotherapies aimed at bolstering the immune system's ability to destroy tumors.

We chose to utilize the hypoxia-activated prodrug [redacted] to disrupt tumor hypoxia. In the presence of hypoxia, [redacted] is reduced to [redacted] leading to the apoptosis of tumor cells[19],[20]. Previous research from our lab illustrated the ability of [redacted] to improve the anti-tumor immune response in immune "cold" prostate tumors by disrupting hypoxic zones[redacted]. We recapitulated this data in the orthotopic GL261 GBM tumor model showing that [redacted] reduces tumor hypoxia and prolongs survival in mice (Figure 1, 2). To ensure this can be recapitulated in another GBM tumor model, we used the orthotopic CT2A GBM model and observed the same results (Figure 2B). Therefore, as we have established the ability to reduce tumor hypoxia using [redacted], it is essential to comprehend the ensuing effects of hypoxia reduction on effector $CD8^+$ T cells and GAMs within the TME.

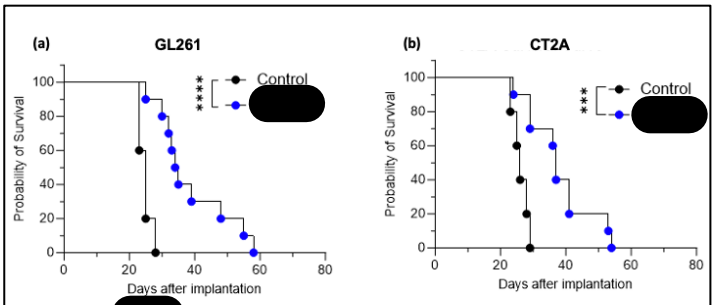

Figure 2: [redacted] treatment enhances survival in GBM mouse models
GL261 (a) and CT2A (b) GBM tumor-bearing mice ($5x10^4$ cells) were treated with 50mg/kg [redacted] on days 10-14, 16-20. Mice were monitored for survival (5-10m/group). Statistical significance for survival was calculated using the log-rank (Mantel-Cox) test.

INNOVATION

There is very little information on the impact of tumor hypoxia reduction on the immune microenvironment, especially in the context of GBM. Research from our lab and others has established the possibility of reducing tumor hypoxia to reinvigorate a "cold" tumor. As a result, this proposal addresses a major gap in our knowledge of the mechanisms driving these effects in GBM by directly assessing cytotoxic $CD8^+$ T cells and GAMs. Additionally, there is very little research on the impact of chronic hypoxia (tumor hypoxia) on immune cells in GBM. Consequently, there is very little information on the differential impact of tumor hypoxia on bone marrow-derived macrophages versus central nervous system-resident microglia. Thus, we will be using the microglia-specific surface marker [redacted] to differentiate between these two populations of GAMs[22]. As a result, this proposal will identify key mechanistic pathways involved in reversing GBM tumor hypoxia, with an emphasis on studying the impact of hypoxia reduction on CNS-resident microglia. Furthermore, there is inadequate information on the impact of tumor hypoxia and tumor hypoxia reduction on $CD8^+$ T cell metabolism in GBM. Therefore, we will identify a gap in knowledge by assessing the impact of hypoxia reduction on the metabolic alterations and subsequent effector functionality of $CD8^+$ T cells. Additionally, we will use the clinically relevant 18F-FAZA PET imaging system to study *in vivo* hypoxia levels within murine GBM. This will enable us to study the effectiveness of hypoxia reduction using the hypoxia-activated prodrug, [redacted]. 18F-FAZA PET imaging allows us to monitor changes in tumor hypoxia in real time and is highly translatable as it has been previously used in the clinic.

APPROACH

Aim 1: Determine the effects of hypoxia reduction on $CD8^+$ T cell distribution, infiltration, and cytotoxicity in GBM.

Prior research has confirmed the presence of a reduced population of functional cytotoxic $CD8^+$ T cells within hypoxic regions of tumors[redacted]. We recapitulated this in the GL261 GBM tumor model where hypoxic niches had a lower number of CD3 T cells (Figure 3). However, the precise mechanisms responsible for this remain unclear. Previous research states that hypoxia induces poor vasculature lacking the necessary adhesion molecules for T cell extravasation and entry into the TME[23],[24]. The T cells that do infiltrate hypoxic regions struggle to endure the metabolically harsh environment and lose their cytotoxic capabilities[25],[26]. Additionally, while we showed that hypoxia reduction using [redacted] could enhance CD3 infiltration into the TME (Figure 3), we do not know if these T cells originate from the tumor periphery, where they might undergo proliferation and migrate into the tumor core, or if there is an increased influx of T cells from the lymph nodes (LNs). Therefore, our objective is to understand the (1) spatiotemporal distribution of $CD8^+$ T cells within the GBM hypoxic TME (2) explore the impact of hypoxia reduction on $CD8^+$ T cell metabolism and functionality within the GBM TME, and (3) study the impact of tumor hypoxia reduction on $CD8^+$ T cell trafficking from the lymph nodes in GBM.

1.1 Characterize the hypoxic niche within the GBM tumor.

To assess the impact of [redacted] on hypoxia reduction *in vivo*, 18F-FAZA PET imaging will be used. $5x10^4$ GL261 cells will be implanted in 20 C57BL/6 mice intracranially via stereotactic implantation surgery. 10 mice will receive

[redacted] (as illustrated in Figure 4), with 10 mice receiving PBS i.p. (control group). 18F-FAZA PET imaging will be done on day 25. Mice will be given an IV injection of 18F-FAZA and PET imaging done 3 hours later. Naïve mice without GBM tumors will be used as a negative control. *In vivo* hypoxia levels will be compared between naïve mice, the control group, and the mice receiving [redacted] treatment. Additionally, mice will be imaged at later time points (days 30 and 35) to look at the persistence of hypoxia reduction following [redacted] treatment.

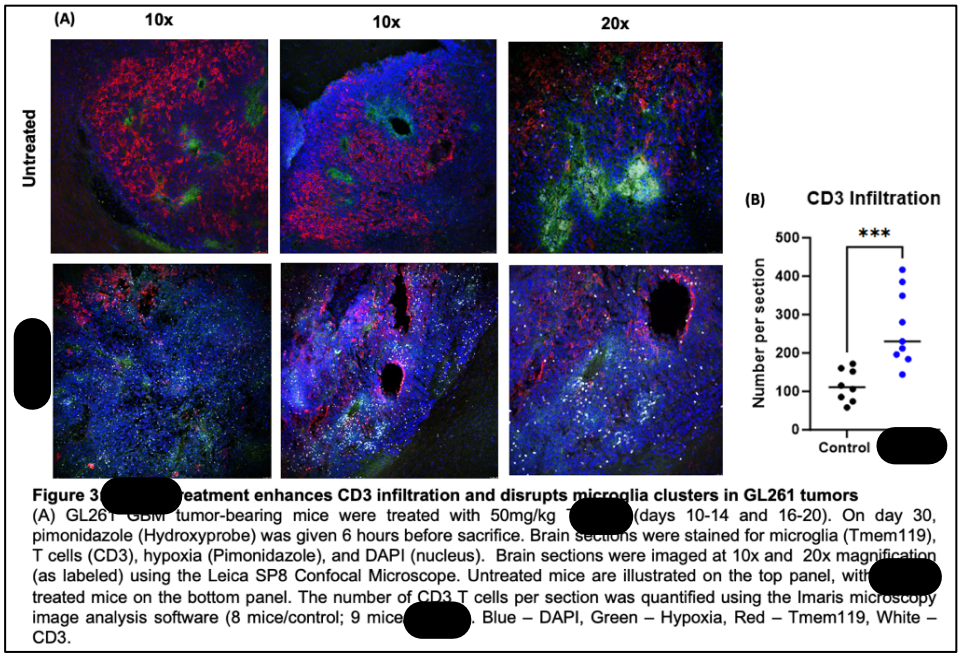

Figure 3[redacted]eatment enhances CD3 infiltration and disrupts microglia clusters in GL261 tumors
(A) GL261 GBM tumor-bearing mice were treated with 50mg/kg [redacted] (days 10-14 and 16-20). On day 30, pimonidazole (Hydroxyprobe) was given 6 hours before sacrifice. Brain sections were stained for microglia (Tmem119), T cells (CD3), hypoxia (Pimonidazole), and DAPI (nucleus). Brain sections were imaged at 10x and 20x magnification (as labeled) using the Leica SP8 Confocal Microscope. Untreated mice are illustrated on the top panel, with [redacted] treated mice on the bottom panel. The number of CD3 T cells per section was quantified using the Imaris microscopy image analysis software (8 mice/control; 9 mice[redacted]. Blue – DAPI, Green – Hypoxia, Red – Tmem119, White – CD3.

We leveraged immunofluorescence imaging to further characterize the spatiotemporal distribution of immune cells in relation to the hypoxic niche. GL261 cells were implanted via stereotactic surgery, with 8 mice receiving [redacted] and 8 mice receiving PBS i.p. (Figure 4). Mice were sacrificed on day 30, with 60mg/kg of pimonidazole given i.p. 6 hours before sacrifice to bind hypoxic adducts. While mice were sacrificed, brains were perfused through transcardiac perfusion. Brain tissues were dissected and embedded in agarose. Agarose-embedded tissues were sliced into 100uM sections using a vibratome. Brain tissues were stained for Pimonidazole (hypoxia), CD3 (T cells), Tmem119 (microglia), and DAPI (nuclei), and imaged using the Leica SP8 Confocal Microscope. Our results indicate that GL261 tumors contain hypoxic niches (green) that are devoid of T cells (white) as illustrated in Figure 3A (top panel). [redacted] treatment drastically reduced tumor hypoxia (green), and enhanced CD3 T cell infiltration (white) as seen in Figure 3A (lower panel). CD3 T cell numbers within tumors were quantified using the Imaris microscopy image analysis software in both untreated and [redacted]-treated mice, with the [redacted] treated tumors having significantly more CD3 infiltration (Figure 3B). To identify the impact of [redacted] treatment on vasculature remodeling we will conduct IF staining for CD31 which marks blood vessels and endothelial cells. Subsequently, CD3/CD31 co-staining would allow us to discern the impact of vasculature remodeling on T cell infiltration.

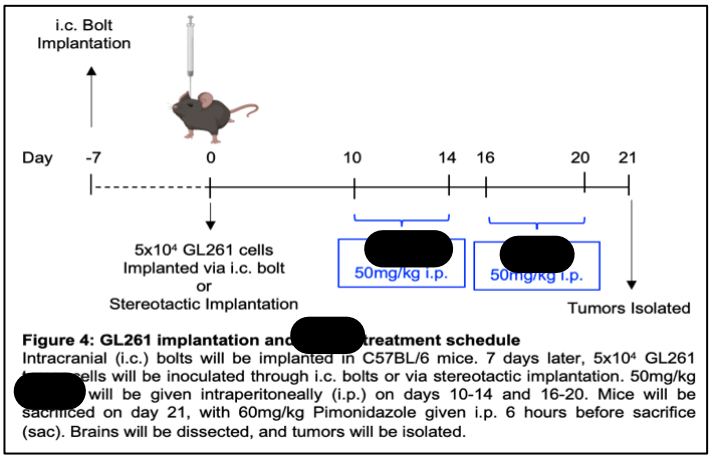

Figure 4: GL261 implantation and [redacted]treatment schedule
Intracranial (i.c.) bolts will be implanted in C57BL/6 mice. 7 days later, 5x10⁴ GL261 [redacted]cells will be inoculated through i.c. bolts or via stereotactic implantation. 50mg/kg [redacted] will be given intraperitoneally (i.p.) on days 10-14 and 16-20. Mice will be sacrificed on day 21, with 60mg/kg Pimonidazole given i.p. 6 hours before sacrifice (sac). Brains will be dissected, and tumors will be isolated.

1.2 Determine the impact of hypoxia reduction on CD8⁺ T cell metabolism and effector potential within the GBM TME.

To identify the impact of [redacted]-mediated hypoxia reduction on the metabolic status of CD8⁺ T cells, a seahorse assay will be used. 9 GL261 tumor-bearing C57BL/6 mice will be treated with [redacted] (Figure 4), and 9 mice treated with PBS i.p. (control group). Brains will be dissected on day 21, and CD8⁺ T cells will be isolated using CD8a magnetic beads. CD8⁺ T cells from 3 mice will be grouped together to account for the low number of CD8⁺ T cells present in GBM tumors (giving a total of 3 groups per condition). The Seahorse XF Cell Mito Stress Test Kit will be used to measure mitochondrial function. 3 serial injections of oligomycin, rotenone, and antimycin A (complex V, I, and III inhibitors) will be done to study basal respiration, ATP-linked respiration, and spare respiratory capacity (SRC).

The impact of hypoxia reduction on CD8⁺ T cell functionality will be assessed by isolating primary tumor-infiltrating lymphocytes (TILs). 10 GL261 tumor-bearing C57BL/6 mice will be treated with [redacted] (Figure 4), and 10 mice treated with PBS (control group). GBM tumors and tumor-draining lymph nodes (cervical LNs) will be isolated on day 21, and 60mg/kg Pimonidazole treatment given 6 hours before sacrifice to bind tumor hypoxia

areas. TILs in the tumor will be separated using percoll gradient centrifugation. Lymphocytes from the tumor and cervical LNs will be stained for markers studying T cell activation, proliferation, cytotoxicity, and exhaustion as described in Table 1. Analysis will be conducted using the BD X-30 flow cytometer and FlowJo software (both of which will be used throughout this proposal). Results will be compared between the control group (no [redacted]) and the experimental group (with [redacted] treatment). Pimonidazole staining will allow us to differentiate between $CD8^+$ T cells under hypoxia (Pimonidazole positive) versus under normoxia (Pimonidazole negative).

	Markers
Activation	CD44 CD137
Proliferation	Ki67
Cytotoxicity	Granzyme B Perforin IFNγ TNFα IL-2
Exhaustion	PD-1 TIM3 LAG3 TIGIT

Table 1: $CD8^+$ T cell functional markers

1.3 Study the effect of hypoxia modulation on $CD8^+$ T cell trafficking and migration from the lymph nodes in GBM.

To determine the source of intratumoral T cells following hypoxia reduction, we will block T cell trafficking from the LNs to identify the subsequent impact on the T cell response in the TME. T cell exit will be blocked using the immunomodulatory drug FTY720, and TILs will be isolated from the tumor. The efficacy of blocking T cell egress will be confirmed by collecting blood samples from mice treated with/without FTY720 and checking for the presence of T cells in circulation via flow cytometry. This experiment will encompass 4 treatment conditions with 10 mice per group: (1) tumor (2) tumor + FTY720 (3) tumor + [redacted] (4) tumor + FTY720 + [redacted]. Respective GL261 tumor-bearing mice will receive [redacted] (Figure 4). Subsequently, 0.3mg/kg of FTY720 i.p. will be given to respective mice every other day starting day 9. This will allow $CD8^+$ T cells to be primed and traffic to the TME while also blocking T cell migration before [redacted] treatment commences on day 10. On day 21, mice will be sacrificed, and GBM tumors dissected to isolate TILs as described above. Analysis of $CD8^+$ T cells within the TME will be conducted by staining for cell markers listed in Table 1 via flow cytometry.

Expected Results and Interpretation

We have established that GBM tumors contain hypoxic niches that are devoid of T cells and that [redacted] can reduce tumor hypoxia to enhance T cell infiltration. We believe that hypoxia reduction will improve tumor vasculature, allowing T cells to infiltrate the TME. Additionally, the favorable TME resulting from hypoxia reduction will enhance $CD8^+$ T cell survival, modifying their metabolic functionality and boosting cytotoxicity. Their cytolytic capabilities will be enhanced by the continual infiltration of T cells from the TdLNs, constantly replenishing the TME with functional $CD8^+$ T cells that can foster sustained anti-tumor immunity.

Pitfalls, and Alternative Approaches

1. If intraperitoneal or intravenous delivery of 18F-FAZA does not penetrate the blood-brain barrier, we will deliver 18F-FAZA through transparent bolts intracranially that will stain hypoxic brain tumor areas and will not interfere with PET imaging.
2. As gliomas can be diffuse, it may be hard to distinguish the margin between healthy brain tissue and tumors across different mice. In this case, we will isolate the whole hemisphere to enhance reliability.
3. Due to the known role of persistent antigen stimulation in driving T cell exhaustion, it is possible that [redacted]-induced tumor killing will exacerbate $CD8^+$ T cell exhaustion. In this case, we will modify the [redacted] treatment plan to either shorten the duration of treatment or extend the intervals between treatments to alleviate T cell exhaustion[27],[28].

<u>Aim 2: Discern the impact of hypoxia reduction on the distribution and polarization of GAMs in GBM.</u>

GAMs account for 50% of the immune milieu in GBM and take on a more M2 immunosuppressive phenotype in the presence of tumor hypoxia[29]–[33]. These immunosuppressive GAMs release cytokines that enhance tumor proliferation and suppress cytotoxic immune cells[34]. Additionally, these resident microglia are unique to the central nervous system, with little differentiation made between microglia and bone marrow-derived macrophages in the literature on tumor hypoxia. GAMs are a strong predictor of survival outcomes in GBM, highlighting the importance of studying them in the context of hypoxia reduction[35]. Therefore, we will focus on studying the impact of GBM hypoxia reduction on the (1) distribution of GAM subtypes (2) its impact on GAM polarization (3) and the subsequent effect of GAM polarization on T cell activity.

2.1 Study the spatiotemporal distribution of GAMs in response to hypoxia modulation.

To study the spatiotemporal distribution of GAMs in relation to tumor hypoxia, we first conducted IF imaging of microglia using the microglia-specific surface marker Tmem119[35]. IF imaging was done as described in Aim 1.1 on GL261 tumor-bearing mice with/without [redacted] treatment. As illustrated in Figure 3, microglia (red) form clusters around a central hypoxic niche, with very little infiltration into hypoxic zones. They also appear ramified which indicates resting-state microglia[22]. Upon hypoxia reduction using [redacted], they become amoeboid-shaped (activated) and infiltrate the tumor, spreading throughout the TME[22]. To further clarify their functionality, we will stain microglia for the M1 marker iNOS and M2 marker CD206 and visualize them using Immunofluorescence (IF) imaging. Additionally, the Imaris microscopy software will be employed to quantitatively assess the prevalence of ramified versus amoeboid microglia within the tumor TME. Furthermore, the distribution of myeloid-derived suppressor cells (MDSCs) will be assessed using IF imaging for Gr-1. To distinguish bone marrow-derived macrophages from microglia, F4/80 and Tmem119 co-staining will be conducted as microglia express both markers while bone marrow-derived macrophages express only F4/80.

2.2 Identify the effect of hypoxia reduction on GAM polarization.

To explore the effect of hypoxia reduction on the phenotype and functionality of the different GAM populations *in vivo*, TIL analysis will be conducted. 10 GL261 tumor-bearing mice will be treated with [redacted] (Figure 4), and 10 mice treated with PBS i.p. (control group). GBM tumors will be isolated on day 21, and 60mg/kg Pimonidazole treatment given 6 hours before sacrifice to bind tumor hypoxia. TILs will be separated using percoll gradient centrifugation and stained for cell markers described in Table 2. Using the phenotypic markers, GAM populations will be differentiated (microglia, monocytic MDSCs, granulocytic MDSCs, and TAMs). Their polarization state will be analyzed using functional markers (M1/M2). Pimonidazole staining will allow us to differentiate between GAMs in normoxia versus hypoxia. GAM phenotype and functionality will be compared between the [redacted] treated group and the control group.

Cell Type	Phenotypic Markers	Gating	M1 Markers	M2 Markers
Microglia	Tmem119	$CD45^{mid} \rightarrow Tmem119^{+}$	CD80 CD86 iNOS	Arginase CD206 CD163 PD-L1
Macrophages	CD11b	$CD45^{hi} \rightarrow CD11b^{+}$		
GrMDSCs	Ly6C /Ly6G	$Ly6G^{hi}\ Ly6C^{mid}$		
Mono-MDSCs	Ly6C /Ly6G	$Ly6C^{hi}\ Ly6G^{lo}$		
TAMs	F4/80	$Ly6C^{lo}\ Ly6G^{lo} \rightarrow F4/80^{+}$		

Table 2: Phenotypic and functional markers to differentiate GAM populations by flow cytometry
Phenotypic markers are listed along with how they will be used to gate on different GAM cell populations. M1 and M2 markers are listed to differentiate between these two functional states. Granulocytic myeloid-derived cells (GrMDSCs); Monocytic myeloid-derived cells (Mono-MDSCs); Tumor-associated macrophages (TAMS)

To identify the mechanisms driving GAM repolarization following [redacted] treatment, the effect of hypoxia reduction on HIF signaling will be examined using bulk RNA-sequencing. 9 GL261 tumor-bearing mice will receive [redacted] (Figure 4), while 9 mice will receive PBS i.p. Tumors will be dissected on day 21, and lymphocytes isolated. 3 mice will be grouped together to enhance GAM cell numbers. GAM cell populations will be separated using a cell sorter (microglia, monocytic MDSCs, granulocytic MDSCs, and TAMs). RNA will be extracted from samples and bulk RNA sequencing conducted in each GAM subtype. Subsequently, special attention will be paid to HIF RNA expression across the GAM subtypes in untreated versus [redacted]-treated mice. This will also enable us to look at the RNA expression of targets downstream of HIF signaling.

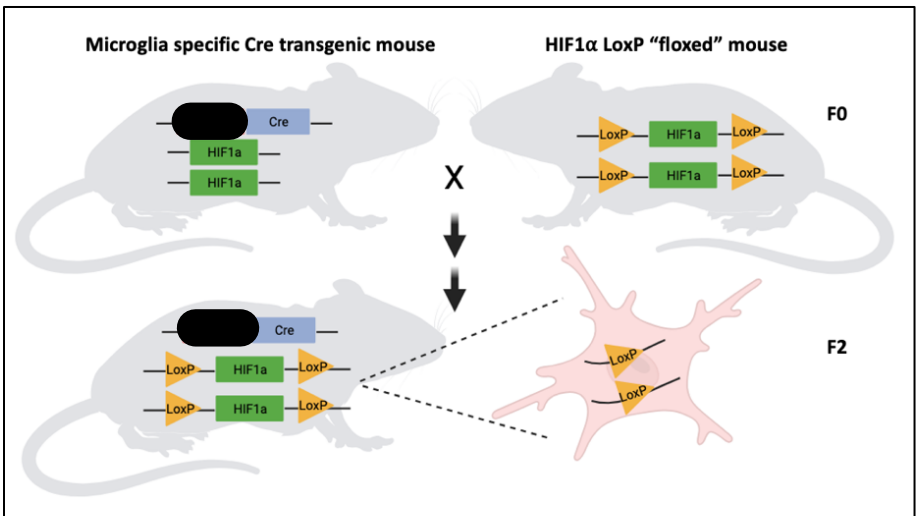

Figure 5: Conditional knockout of HIF1α in [redacted]
A[redacted] transgenic mouse will be bred to a HIF1α homozygous *loxP*-flanked mouse (F0). Approximately 50% of the offspring will be heterozygous for the LoxP allele and heterozygous for the Cre transgene (F1 not shown). These mice will be mated back to the homozygous loxP-flanked mice. Approximately 25% of the progeny from this mating will be homozygous for the loxP-flanked allele and heterozygous for the Cre transgene (F2). These are the experimental mice.

Furthermore, to establish the importance of HIF signaling in GAM repolarization, we will use mice that have a myeloid-specific knockout of HIF1α or HIF2α. $HIF1\alpha^{flox/flox}$ and $HIF2\alpha^{flox/flox}$ mice have a conditional knockout of HIF1α or HIF2α gene using Cre-loxP technology. Concurrently, lysozyme M (LysM) Cre mice have Cre recombinase under the control of the lysozyme promoter that is myeloid-

specific. However, as LysM may target only bone marrow-derived macrophages, [redacted] mice will also be used that have a Cre recombinase under the control of the microglia-specific surface marker [redacted]. HIF1α$^{flox/flox}$ and HIF2α$^{flox/flox}$ mice were crossed with LysM Cre mice to selectively delete HIF1α or HIF2α in all myeloid cells (currently have). Additionally, HIF1α$^{flox/flox}$ and HIF2α$^{flox/flox}$ mice will be crossed with [redacted] mice to selectively delete HIF1α or HIF2α in microglia. Figure 5 illustrates how HIF1α will be knocked out in microglia. The same will be done using HIF2α LoxP mice. GL261 cells will be implanted in wildtype, HIF1α$^{flox/flox}$ - LysM Cre, HIF2α$^{flox/flox}$- LysM Cre, HIF1α$^{flox/flox}$ – [redacted], and HIF2α$^{flox/flox}$- [redacted] mice (10 mice per group). 5 mice per group will be treated with [redacted] and 5 mice treated with PBS i.p. (Figure 4). GBM tumors will be isolated on day 21 and GAM phenotypes and functionality assessed using flow cytometry (Table 2). By comparing the results obtained from wildtype mice versus conditional knockout mice with/without [redacted], we will identify the importance of the HIF pathway in mediating GAM polarization following hypoxia reduction.

2.3 Investigate the impact of GAM polarization on subsequent T cell activity.

To study the direct impact of GAM polarization on CD8$^+$ T cells, an *ex vivo* T cell suppression assay will be done. GL261 OVA cells (5x10^4 IC) will be implanted in 18 C57BL/6 mice. 9 mice will be treated with [redacted] (Figure 4), and 9 mice treated with PBS i.p. Tumors will be isolated on day 21, and GAMs separated using a cell sorter to differentiate microglia, monocytic MDSCs, granulocytic MDSCs, and TAMs. 3 mice per group will be pooled together to account for low cell numbers. Concurrently, CD8$^+$ T cells will be isolated from the naïve spleen of an OT-1 mouse using CD8a magnetic bead separation. CFSE-labeled T cells will be co-cultured with the different GAM populations. CD8$^+$ T cells will be analyzed using flow cytometry 72 hours later for phenotypic and functional markers (proliferation: CFSE, cytotoxicity: granzyme B and perforin, exhaustion – PD-1, TIM3, LAG3, activation – CD44) and intracellular cytokines (IFNγ, TNFα, IL-2).

To identify mechanisms on how GAMs influence T cells, primary sorted GAM populations from the experiment above will also be analyzed via flow cytometry. They will be stained for the following markers/cytokines linked to T cell suppression under hypoxia: VISTA and PD-L1 (inhibitory markers), arginase (depletes arginine), Indoleamine 2,3 dioxygenase - IDO (depletes tryptophan), CD39 and CD73 (produces adenosine) and TGFβ, IL-10 (inhibitory cytokines). This will enable us to identify the impact of hypoxia-mediated GAM repolarization on antigen-specific CD8$^+$ T cell suppression and the pathways involved.

Expected Results and Interpretation

Our preliminary results show that microglia form clusters around hypoxic niches, with hypoxic reduction diffusing these clusters, allowing them to infiltrate the tumor (Figure 3). We anticipate that this will occur for other GAM subsets as well. We predict hypoxia reduction repolarizes M2 GAMs to a pro-inflammatory M1 phenotype by reducing HIF activity. Subsequently, the pro-inflammatory repolarization of GAMs will have lower numbers of inhibitory molecules capable of suppressing CD8$^+$ T cells, leading to enhanced CD8$^+$T cell activation and proliferation.

Expected Pitfalls, and Alternative Approaches

1. The effects of [redacted] treatment on the *in vivo* polarization of GAMs may demonstrate dynamic changes, making it challenging to capture their phenotype and functionality at a single time point. To overcome this, we can conduct IF imaging at multiple time points to observe fluctuations in spatiotemporal distribution and morphology. Moreover, we can isolate GAMs at various time points post-treatment for further analysis.

CONCLUSION

The completion of this projection is anticipated to unveil a significant gap in our knowledge regarding the influence of tumor hypoxia on the immune cell milieu in GBM. This investigation will shed light on a pivotal concept— the potential utility of hypoxia-activated prodrugs such as [redacted]—as a strategy to mitigate tumor hypoxia and, consequently, as an immune-potentiating intervention for GBM. Furthermore, it will identify key molecular mechanisms underlying cellular responses to hypoxia that will not only enhance our understanding of tumor hypoxia in GBM but also offer insights into potential novel therapeutic targets.

REFERENCES

[1] L. Yang, C. Lin, L. Wang, H. Guo, and X. Wang, “Hypoxia and hypoxia-inducible factors in glioblastoma multiforme progression and therapeutic implications.,” *Exp Cell Res*, vol. 318, no. 19, pp. 2417–26, Nov. 2012, doi: 10.1016/j.yexcr.2012.07.017.

[2] M. E. Davis, “Glioblastoma: Overview of Disease and Treatment.,” *Clin J Oncol Nurs*, vol. 20, no. 5 Suppl, pp. S2-8, Oct. 2016, doi: 10.1188/16.CJON.S1.2-8.

[3] S. Jawhari, M.-H. Ratinaud, and M. Verdier, “Glioblastoma, hypoxia and autophagy: a survival-prone ‘ménage-à-trois’.,” *Cell Death Dis*, vol. 7, no. 10, p. e2434, Oct. 2016, doi: 10.1038/cddis.2016.318.

[4] R. Vuillefroy de Silly, P.-Y. Dietrich, and P. R. Walker, “Hypoxia and antitumor CD8+ T cells: An incompatible alliance?,” *Oncoimmunology*, vol. 5, no. 12, p. e1232236, 2016, doi: 10.1080/2162402X.2016.1232236.

[5] A. Sattiraju *et al.*, “Hypoxic niches attract and sequester tumor-associated macrophages and cytotoxic T cells and reprogram them for immunosuppression.,” *Immunity*, vol. 56, no. 8, pp. 1825-1843.e6, Aug. 2023, doi: 10.1016/j.immuni.2023.06.017.

[6] S. Huang *et al.*, “Assessment of tumor hypoxia and perfusion in recurrent glioblastoma following bevacizumab failure using MRI and 18F-FMISO PET.,” *Sci Rep*, vol. 11, no. 1, p. 7632, Apr. 2021, doi: 10.1038/s41598-021-84331-5.

[7] R. Du *et al.*, “HIF1alpha induces the recruitment of bone marrow-derived vascular modulatory cells to regulate tumor angiogenesis and invasion.,” *Cancer Cell*, vol. 13, no. 3, pp. 206–20, Mar. 2008, doi: 10.1016/j.ccr.2008.01.034.

[8] S. Y. Leung, M. P. Wong, L. P. Chung, A. S. Chan, and S. T. Yuen, “Monocyte chemoattractant protein-1 expression and macrophage infiltration in gliomas.,” *Acta Neuropathol*, vol. 93, no. 5, pp. 518–27, May 1997, doi: 10.1007/s004010050647.

[9] A. Casazza *et al.*, “Impeding macrophage entry into hypoxic tumor areas by Sema3A/Nrp1 signaling blockade inhibits angiogenesis and restores antitumor immunity.,” *Cancer Cell*, vol. 24, no. 6, pp. 695–709, Dec. 2013, doi: 10.1016/j.ccr.2013.11.007.

[10] M. Z. Noman *et al.*, “Hypoxia: a key player in antitumor immune response. A Review in the Theme: Cellular Responses to Hypoxia.,” *Am J Physiol Cell Physiol*, vol. 309, no. 9, pp. C569-79, Nov. 2015, doi: 10.1152/ajpcell.00207.2015.

[11] G. L. Semenza, “HIF-1 inhibitors for cancer therapy: from gene expression to drug discovery.,” *Curr Pharm Des*, vol. 15, no. 33, pp. 3839–43, 2009, doi: 10.2174/138161209789649402.

[12] G. L. Semenza, “Hypoxia-inducible factors in physiology and medicine.,” *Cell*, vol. 148, no. 3, pp. 399–408, Feb. 2012, doi: 10.1016/j.cell.2012.01.021.

[13] F. O. Martinez, A. Sica, A. Mantovani, and M. Locati, “Macrophage activation and polarization.,” *Front Biosci*, vol. 13, pp. 453–61, Jan. 2008, doi: 10.2741/2692.

[14] C. Riera-Domingo *et al.*, “Immunity, Hypoxia, and Metabolism-the Ménage à Trois of Cancer: Implications for Immunotherapy.,” *Physiol Rev*, vol. 100, no. 1, pp. 1–102, Jan. 2020, doi: 10.1152/physrev.00018.2019.

[15] V. Pietrobon and F. M. Marincola, “Hypoxia and the phenomenon of immune exclusion.,” *J Transl Med*, vol. 19, no. 1, p. 9, Jan. 2021, doi: 10.1186/s12967-020-02667-4.

[16] N. E. Scharping *et al.*, “The Tumor Microenvironment Represses T Cell Mitochondrial Biogenesis to Drive Intratumoral T Cell Metabolic Insufficiency and Dysfunction.,” *Immunity*, vol. 45, no. 2, pp. 374–88, Aug. 2016, doi: 10.1016/j.immuni.2016.07.009.

[17] C.-H. Chang *et al.*, “Metabolic Competition in the Tumor Microenvironment Is a Driver of Cancer Progression.,” *Cell*, vol. 162, no. 6, pp. 1229–41, Sep. 2015, doi: 10.1016/j.cell.2015.08.016.

[18] N. E. Scharping *et al.*, “The Tumor Microenvironment Represses T Cell Mitochondrial Biogenesis to Drive Intratumoral T Cell Metabolic Insufficiency and Dysfunction.,” *Immunity*, vol. 45, no. 2, pp. 374–88, Aug. 2016, doi: 10.1016/j.immuni.2016.07.009.

[19] J. D. Sun *et al.*, “Comparison of hypoxia-activated prodrug evofosfamide (TH-302) and ifosfamide in preclinical non-small cell lung cancer models.,” *Cancer Biol Ther*, vol. 17, no. 4, pp. 371–80, Apr. 2016, doi: 10.1080/15384047.2016.1139268.

[20] A. Brenner *et al.*, “Hypoxia-activated evofosfamide for treatment of recurrent bevacizumab-refractory glioblastoma: a phase I surgical study.,” *Neuro Oncol*, vol. 20, no. 9, pp. 1231–1239, Aug. 2018, doi: 10.1093/neuonc/noy015.

[21] [redacted]

[22] [redacted]

[23] G. T. Motz *et al.*, “Tumor endothelium FasL establishes a selective immune barrier promoting tolerance in tumors.,” *Nat Med*, vol. 20, no. 6, pp. 607–15, Jun. 2014, doi: 10.1038/nm.3541.

[24] S. Chouaib, M. Z. Noman, K. Kosmatopoulos, and M. A. Curran, “Hypoxic stress: obstacles and opportunities for innovative immunotherapy of cancer.,” *Oncogene*, vol. 36, no. 4, pp. 439–445, Jan. 2017, doi: 10.1038/onc.2016.225.

[25] Y. G. Najjar *et al.*, “Tumor cell oxidative metabolism as a barrier to PD-1 blockade immunotherapy in melanoma.,” *JCI Insight*, vol. 4, no. 5, Mar. 2019, doi: 10.1172/jci.insight.124989.

[26] C.-H. Chang *et al.*, “Metabolic Competition in the Tumor Microenvironment Is a Driver of Cancer Progression.,” *Cell*, vol. 162, no. 6, pp. 1229–41, Sep. 2015, doi: 10.1016/j.cell.2015.08.016.

[27] S. D. Blackburn, H. Shin, G. J. Freeman, and E. J. Wherry, “Selective expansion of a subset of exhausted CD8 T cells by alphaPD-L1 blockade.,” *Proc Natl Acad Sci U S A*, vol. 105, no. 39, pp. 15016–21, Sep. 2008, doi: 10.1073/pnas.0801497105.

[28] S. Kumar *et al.*, “Hypoxia-Targeting Drug Evofosfamide (TH-302) Enhances Sunitinib Activity in Neuroblastoma Xenograft Models.,” *Transl Oncol*, vol. 11, no. 4, pp. 911–919, Aug. 2018, doi: 10.1016/j.tranon.2018.05.004.

[29] C. Xu *et al.*, “Origin, activation, and targeted therapy of glioma-associated macrophages.,” *Front Immunol*, vol. 13, p. 974996, 2022, doi: 10.3389/fimmu.2022.974996.

[30] J. Xu *et al.*, “Hypoxic glioma-derived exosomes promote M2-like macrophage polarization by enhancing autophagy induction.,” *Cell Death Dis*, vol. 12, no. 4, p. 373, Apr. 2021, doi: 10.1038/s41419-021-03664-1.

[31] X. Guo *et al.*, “Hypoxia promotes glioma-associated macrophage infiltration via periostin and subsequent M2 polarization by upregulating TGF-beta and M-CSFR.,” *Oncotarget*, vol. 7, no. 49, pp. 80521–80542, Dec. 2016, doi: 10.18632/oncotarget.11825.

[32] M. M. Leblond *et al.*, “Hypoxia induces macrophage polarization and re-education toward an M2 phenotype in U87 and U251 glioblastoma models.,” *Oncoimmunology*, vol. 5, no. 1, p. e1056442, 2016, doi: 10.1080/2162402X.2015.1056442.

[33] G. Zhang, X. Tao, B. Ji, and J. Gong, “Hypoxia-Driven M2-Polarized Macrophages Facilitate Cancer Aggressiveness and Temozolomide Resistance in Glioblastoma.,” *Oxid Med Cell Longev*, vol. 2022, p. 1614336, 2022, doi: 10.1155/2022/1614336.

[34] G. Wang *et al.*, “Tumor-associated microglia and macrophages in glioblastoma: From basic insights to therapeutic opportunities.,” *Front Immunol*, vol. 13, p. 964898, 2022, doi: 10.3389/fimmu.2022.964898.

[35] A. A. Thomas *et al.*, “Regulatory T cells are not a strong predictor of survival for patients with glioblastoma.,” *Neuro Oncol*, vol. 17, no. 6, pp. 801–9, Jun. 2015, doi: 10.1093/neuonc/nou363.